

Direct Model Reference Adaptive Control of Permanent Magnet Brushless DC Motors

Yilmaz Sozer*

Howard Kaufman**

David A. Torrey*

*Department of Electric Power Engineering, Rensselaer Polytechnic Institute
Troy, NY 12180-3590, Voice: (518) 276-8297, Fax: (518) 276-6226

**Department of Electric Computer and Systems Engineering, Rensselaer Polytechnic Institute
Troy, NY 12180-3590

sozery@rpi.edu , kaufmh@rpi.edu , torred@rpi.edu

Abstract

A direct model reference adaptive control (DMRAC) algorithm is applied to the speed control of an inverter driven permanent magnet brushless dc motor. The approximation of the nonlinear system, current limitation and the parameter changes are addressed during the development of this controller. The control is described as an outer loop speed control and an inner current loop control which has faster dynamics than the speed loop. The adaptive control is applied to the outer speed control loop. DMRAC is compared to an indirect adaptive controller and a standard PI controller. Simulation results show that the two adaptive controllers give similar response and are superior to the PI controller. However, the DMRAC algorithm is simpler to implement.

1. Introduction

Permanent magnet brushless dc (PMBDC) motors are becoming popular with continued cost reductions and performance improvements in permanent magnet materials. The main advantages of the PMBDC motor are the high efficiency, high power density and the low maintenance cost due to the removal of the brushes [1], [2].

This paper focuses on the direct model reference adaptive control (DMRAC) of the PMBDC motor. Indirect model reference adaptive controller (IMRAC) and a conventional PI controller are used to emphasize DMRAC features. The main objective is to achieve precise speed control in the face of varying motor parameters and load. Most of the work on adaptive control of permanent magnet motors has been done with indirect methods which need parameter estimation [3]; however DMRAC has been successfully applied to induction machines [4].

The main problem in DMRAC occurs during large transients where the inverter cannot provide the current demanded by the adaptive controller. Although small gains solve the problem, they cause weakness in the adaptability of the controller during the parameter changes. An incremental steps technique is proposed to alleviate this

problem and is successfully applied to the DMRAC algorithm.

The time scale difference between the electrical and mechanical dynamics enables us to use multiloop motor control [3]. The outer speed loop is controlled adaptively in the face of varying motor parameters and load. Hysteresis current control is used in the inner current loop to shape the motor currents as commanded by the adaptive controller. Fig. 1 shows the control diagram of the PMBDC motor.

Section 2 presents the model and the constraints for PMBDC motors. The DMRAC algorithm used in this paper is described in Section 3. Section 4 describes the algorithm used for IMRAC. Results with representative parameter changes are shown in Section 5. Conclusions and recommendations are in Section 6.

2. Modelling of PMBDC motor

The PMBDC motor consists of stationary 3-phase stator windings and permanent magnets on the rotor. Stator phases are driven by an inverter to supply the motor with a current waveform that produces constant torque during regions of constant back emf. The back emf waveforms have trapezoidal shapes as shown in Fig. 2 with amplitudes of E_s and flat tops widths greater than 120 degrees. The phase current waveforms have quasi-square wave shapes as shown in Fig. 2 with magnitudes of I_s , the control signal, to get a constant torque. The active stator coils are switched every 60 electrical degrees, with one phase turning on or turning off. The electrical position is defined such that movement of the rotor by 360 electrical degrees brings the machine to an identical magnetic orientation [1]. The torque is given by [5], [6]

$$T_e = \frac{e_a i_a + e_b i_b + e_c i_c}{\omega} \quad (1)$$

where e_a , e_b and e_c are the phase back emf voltages, i_a , i_b and i_c are the stator phase currents, and ω is the mechanical speed. With the current waveshape and the back

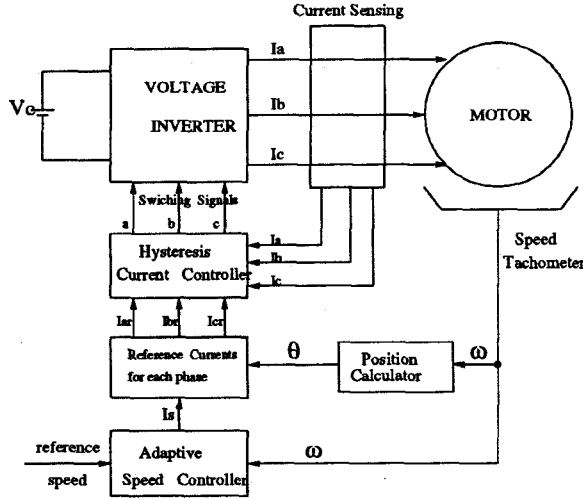


Figure 1: The control diagram of the PMBDC motor.

emfs as in Fig. 2, the torque equation reduces to

$$T_e = \frac{2E_s I_s}{\omega} \quad (2)$$

Defining K_v as the back emf constant with

$$E_s = K_v \omega \quad (3)$$

T_e can be written as

$$T_e = 2K_v I_s \quad (4)$$

so the mechanical dynamics can be written as

$$J \frac{d\omega}{dt} = 2K_v I_s - T_l - B\omega \quad (5)$$

The adaptive controller is applied to this state equation as an outer speed loop. ω is the speed output of the motor, I_s is the control input, J , B and T_l are inertia, viscous damping and load torque, respectively. J , B and T_l are the varying parameters for which we seek control insensitivity. We have to shape the phase currents properly to justify this approximation. That is, phase currents must be quasi-square waves with the magnitude of I_s , as in Fig. 2. A hysteretic current regulator is used to actively shape the phase currents through the electrical dynamics

$$\frac{di_x}{dt} = \left(\frac{1}{L-M} \right) [v_x - Ri_x - e_x] \quad (6)$$

where v_x is the inverter voltage applied to stator phase x ($x = a, b, \text{ or } c$) L is the phase inductance and M is the mutual inductance. The hysteretic controller forces the motor currents i_x ($x = a, b, \text{ or } c$) to approximately follow the reference currents i_{ar} , i_{br} and i_{cr} .

The amplitude of the reference currents is I_s as commanded by the adaptive controller, and their signs are the

same as the signs of the corresponding back emf voltages. The phase of the current is calculated by integrating the speed from the speed tachometer. v_a , v_b and v_c are pulses of magnitude $+V_c$ and $-V_c$. $+V_c$ is applied when the actual current is smaller than the reference current; $-V_c$ is applied in the reverse case. Figure 3 shows the actual motor phase current and the applied voltage to the motor from the inverter.

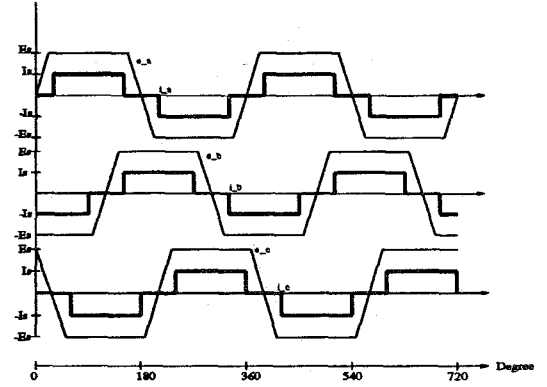


Figure 2: The ideal three phase stator currents and back emfs.

The physical inverter has some limitations. One limitation that we must consider is the maximum current. The current commanded from the adaptive controller must be within specified limits. This issue is discussed further in Section 3.

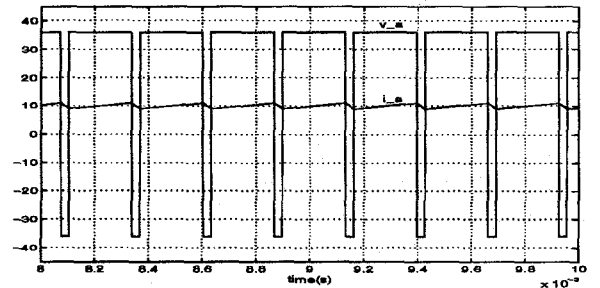


Figure 3: The actual phase current and the voltage applied to this phase.

3. DMRAC Algorithm

The actual DMRAC algorithm is discussed first in Section 3.1. Its application to the PMBDC is then detailed in Section 3.2.

3.1. General algorithm

The linear time invariant model reference adaptive control problem is considered for the plant

$$\begin{aligned} \dot{x}_p(t) &= A_p x_p(t) + B_p u_p(t) \\ y_p(t) &= C_p x_p(t) \end{aligned} \quad (7)$$

where $x_p(t)$ is the $(n \times 1)$ state vector, $u_p(t)$ is the $(m \times 1)$ control vector, $y_p(t)$ is the $(q \times 1)$ plant output vector, and A_p, B_p are matrices with appropriate dimensions. The range of the plant parameters is assumed to be known and bounded with

$$\begin{aligned} \underline{a}_{ij} &\leq a_p(i, j) \leq \bar{a}_{ij}, i, j = 1, \dots, n \\ \underline{b}_{ij} &\leq b_p(i, j) \leq \bar{b}_{ij}, i, j = 1, \dots, n \end{aligned} \quad (8)$$

The objective is to find, without explicit knowledge of A_p and B_p , the control $u_p(t)$ such that the plant output vector $y_p(t)$ follows the reference model

$$\begin{aligned} \dot{x}_m(t) &= A_m x_m(t) + B_m u_m(t) \\ y_m(t) &= C_m x_m(t) \end{aligned} \quad (9)$$

The output y_m is the desired speed response ω to the speed set point command u_m . The model incorporates the desired behavior of the plant, but its choice is not restricted. In particular, the order of the plant may be much larger than the order of the reference model.

The ideal control law that generates perfect output tracking and ideal state trajectories is assumed to be a linear combination of the model states and model input, i.e.

$$\begin{bmatrix} x_p^* \\ u_p^* \end{bmatrix} = \begin{bmatrix} S_{11} & S_{12} \\ S_{21} & S_{22} \end{bmatrix} \begin{bmatrix} x_m(t) \\ u_m(t) \end{bmatrix} \quad (10)$$

where the S_{ij} matrices satisfy

$$\begin{aligned} S_{11}A_m &= A_p S_{11} + B_p S_{21} \\ S_{11}B_m &= A_p S_{12} + B_p S_{22} \\ C_m &= C_p S_{11} \\ 0 &= C_p S_{12} \end{aligned} \quad (11)$$

Then the adaptive control law based on this command generator tracker (CGT) approach is given as [7]

$$u_p(t) = K_e(t)e_y(t) + K_x(t)x_m(t) + K_u(t)u_m(t) \quad (12)$$

where $e_y(t) = y_m(t) - y_p(t)$ and $K_e(t)$, $K_x(t)$, and $K_u(t)$ are adaptive gains and concatenated into the matrix $K(t)$ as

$$K(t) = [K_e(t) \quad K_x(t) \quad K_u(t)] \quad (13)$$

Defining the vector $r(t)$ as

$$r(t) = \begin{bmatrix} y_m(t) - y_p(t) \\ x_m(t) \\ u_m(t) \end{bmatrix}, \quad (14)$$

the control $u_p(t)$ is written in a compact form as

$$u_p(t) = K(t)r(t) \quad (15)$$

where

$$\begin{aligned} K(t) &= K_p(t) + K_i(t) \\ K_p(t) &= [y_m(t) - y_p(t)]r^T(t)T_p, \quad T_p \geq 0 \\ \dot{K}_i(t) &= [y_m(t) - y_p(t)]r^T(t)T_i, \quad T_i > 0 \end{aligned} \quad (16)$$

The sufficiency conditions for asymptotic tracking are:

1. There exists a solution to the CGT problem (11).
2. The plant is almost strictly positive real (ASPR); that is there exists a positive definite constant gain matrix K_e , not needed for implementation, such that the closed loop transfer function

$$G(s) = [I + G_p(s)K_e]^{-1}G_p(s) \quad (17)$$

is strictly positive real (SPR).

The block diagram of the DMRAC is shown in Fig. 4.

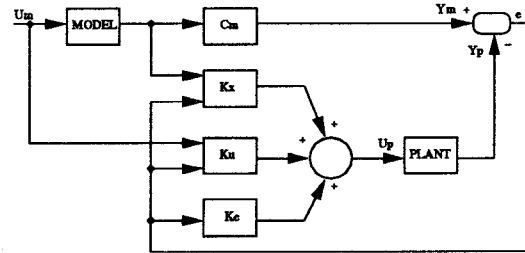


Figure 4: A block diagram for the direct model reference adaptive controller.

3.2. Application to PMBDC

Because the inner current loop has dynamics that are much faster than the outer speed control loop, the adaptive control design is based only upon Eq. 5 with Eq. 6 ignored. However, the evaluation is performed using the entire set of dynamics, which are in fact nonlinear.

In terms of the development in Section 3.1, the state x_p and output y_p are each equal to the speed ω , and the adaptive control u_p is the current magnitude I_s . Comparing Eqs. 5 and 7 indicates that

$$A_p = -\frac{B}{J} \quad (18)$$

$$B_p = \frac{2K_v}{J} \quad (19)$$

The disturbance $(-\frac{T_l}{J})$ is treated as unknown.

The reference model is chosen taking into account the following specifications:

$$98\% \text{ settling time} = 0.4\text{sec} \quad (20)$$

$$\text{Maximum overshoot} = 1\% \quad (21)$$

$$u_p \leq 4A \quad (22)$$

In order to alleviate control saturation, u_r is reduced when u_p is in saturation. Instead of a full step command to the model, u_r is effectively reduced by a series of smaller incremental steps. This algorithm can be summarized as

$$\text{If } u_p > i_{max} \implies u_r = u_s - K(u_p - i_{max}) \quad (23)$$

$$\text{If } u_p \leq i_{max} \implies u_r = u_s, \quad (24)$$

where i_{max} is the maximum limit of current, u_s is the reference speed that we desire, and K is a constant that is found experimentally.

4. IMRAC Algorithm

Indirect model reference adaptive controller (IMRAC) can be summarized as the redesign of the controller based on new estimated parameters to satisfy model tracking and the regulation [8], [9].

A block diagram for the IMRAC system is shown in Fig. 5. This system uses recursive least squares parameter estimator to fit the assumed motor model to the measured performance of the motor. A forgetting factor is used in the parameter estimator to place emphasis on newly required data.

Using the estimated model parameters, the controller is redesigned in order to keep the closed loop poles in a specified location. The controller redesign is represented in Fig. 5 by the three blocks with emerging diagonal arrows. The implementation of the IMRAC is digital, where controller redesign is based on an approximate discrete model. The digital controller then excites a nonlinear continuous time motor model.

The sampled-data form of the continuous motor dynamics given in Eq. 5 is

$$w[k] = bi[k - 1] + aw[k - 1] - cT_l[k - 1] \quad (25)$$

where $a = 1 - \frac{B}{J}T_s$, $b = \frac{2K}{J}T_s$, and $c = \frac{T_r}{J}$. Since it is difficult to measure load T_l and for the purpose of simplifying the controller design, we remove the torque load from the speed equation. The adaptive system accounts for varying load torque by incorporating into the updated parameters a and b .

So our system polynomials became $A(z^{-1}) = 1 - az^{-1}$ and $B(z^{-1}) = b$. The IMRAC control design uses the same performance objectives as the DMRAC system. We chose $C_1(z^{-1}) = 1 - 0.8521z^{-1}$, $C_2(z^{-1}) = 1 + 0.1z^{-1}$ and $D(z^{-1}) = 0.14794$ to satisfy these specifications. Based on these selections the controller blocks become $R(z^{-1}) = a + 0.1$, $B_s(z^{-1}) = 0$ and $b_0 = b$. a and b are the system parameters that need to be estimated.

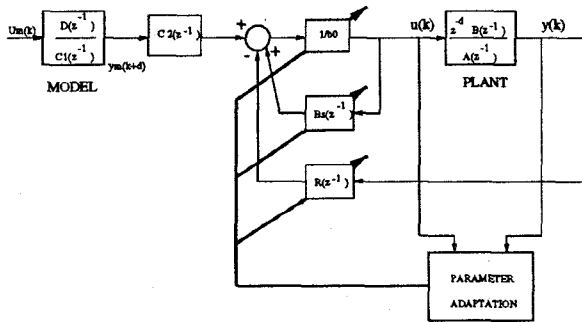


Figure 5: A block diagram for the indirect model reference adaptive controller.

5. Simulation Results

Using a nonlinear model for a PMBDC the performance of the DMRAC, IMRAC and the PI controllers

were tested with three different parameter sets :

$$\text{Set 1 : } J = 0.0015250, B = 0.000801500, T_l = 0.2 \quad (26)$$

$$\text{Set 2 : } J = 0.0007625, B = 0.000601125, T_l = 0.2 \quad (27)$$

$$\text{Set 3 : } J = 0.0007625, B = 0.000601625, T_l = 0.4 \quad (28)$$

The rest of the system parameters are in the Appendix. The transfer function of the PI controller can be written as

$$G_c(s) = \left[\frac{K_P s + K_I}{s} \right] \quad (29)$$

where K_P and K_I were adjusted for the nominal parameters given in Appendix to satisfy the system specifications given in Eqs. 20, 21, 22 ($K_P = 0.1$, $K_I = 0.085$). The system responses of the PI controller for different parameter sets with hysteretic controller are shown in Figs. 6 and 7. It should be noted that the settling time constraint was violated by curves 2 and 3 in Fig. 6; furthermore, a steady state error exists for the same curves.

Figures 8 and 9 document operation of the DMRAC without current limiting for the nominal parameter set, and Figs. 10, 11 and 12 document the operation of the DMRAC with current limiting ($K = 2000$). It should be noted that the current limitation procedure defined by (23) and (24) results in currents that are within the specification (22) and that in both cases, the speed responses are acceptable. The DMRAC with the current limiting procedure was next tested using the three parameter sets defined in Eqs. 26, 27, 28. As shown in Fig. 13, DMRAC (unlike the PI controller) satisfied the specified constraints for all three parameter sets.

We can see little spikes on the current waveforms in DMRAC (Fig. 12) which IMRAC (Fig. 14) and PI controller (Fig. 7) do not have. Although they do not affect the speed response much, these spikes help to reduce ripple on the electromagnetic torque because of the inverter nonlinearities.

Figures 14 and 15 document the operation of the IMRAC, indicating compliance with the performance specifications.

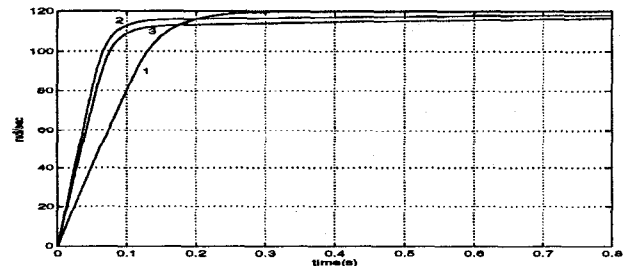


Figure 6: Curve 1 shows the speed response for a PI controller with the parameters Set 1. Curve 2 shows the speed response for a PI controller with the parameters Set 2. Curve 3 shows the speed response for a PI controller with the parameters Set 3.

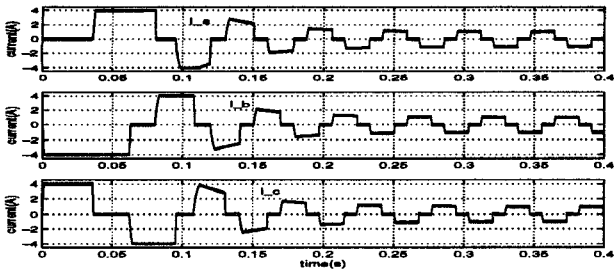


Figure 7: Three phase motor currents using the PI controller with parameter Set 1.

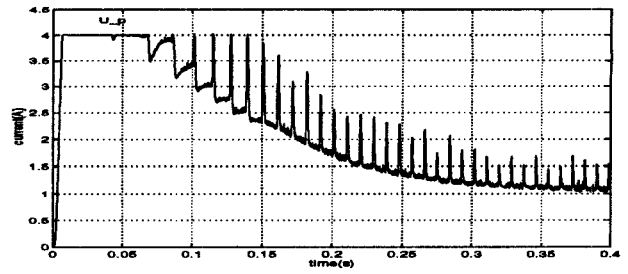


Figure 11: Current commanded from DMRAC with current limiting and with parameter Set 1.

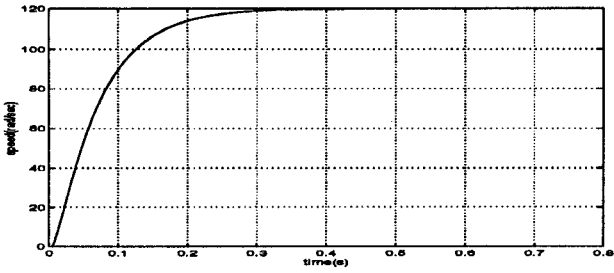


Figure 8: Speed response from DMRAC without current limiting and with parameter Set 1.

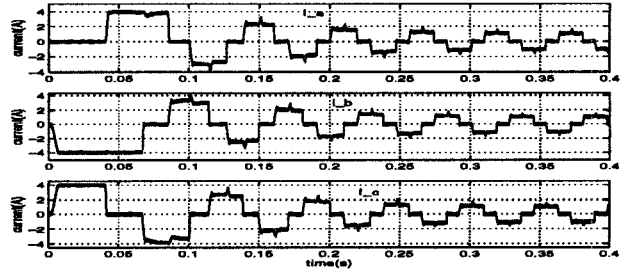


Figure 12: Three phase motor currents from DMRAC with current limiting and with parameter Set 1.

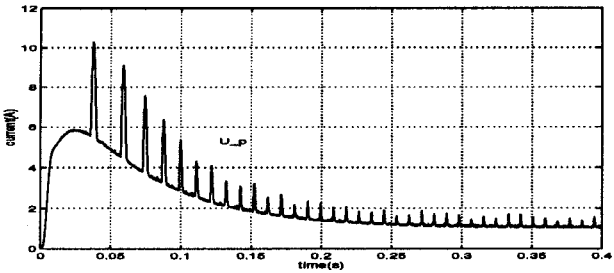


Figure 9: Current commanded from DMRAC without current limiting and with parameter Set 1.

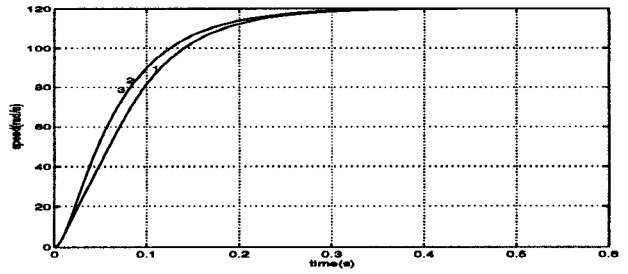


Figure 13: Curve 1 shows the speed response for a DMRAC with parameter Set 1. Curve 2 shows the speed response for a DMRAC with parameter Set 2. Curve 3 shows the speed response for a DMRAC with parameter Set 3.

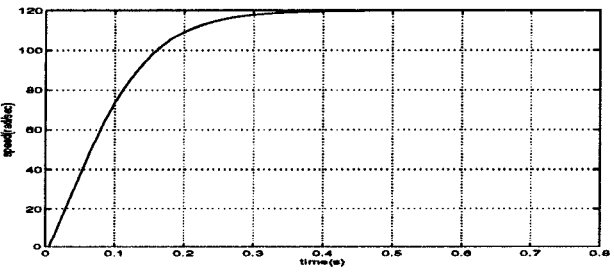


Figure 10: Speed response from DMRAC with current limiting and with parameter Set 1.

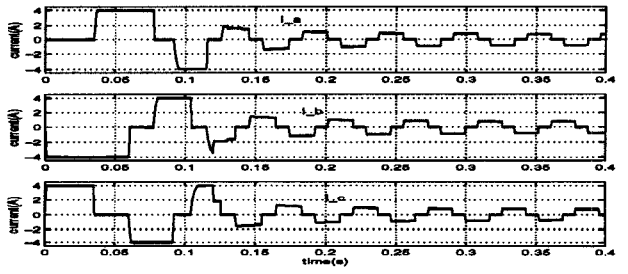


Figure 14: Three phase motor currents using the IMRAC controller with parameter Set 1.

Table 1: Controller Evaluation

Criterion	PI	DMRAC	IMRAC
Adaptability	-	+	+
Start up tuning	+	0	+
Response to Load Variations	-	+	+
Response to Setpoint Changes	+	+	+
Small sample Rates	+	+	-
Complexity of the controller	+	0	-

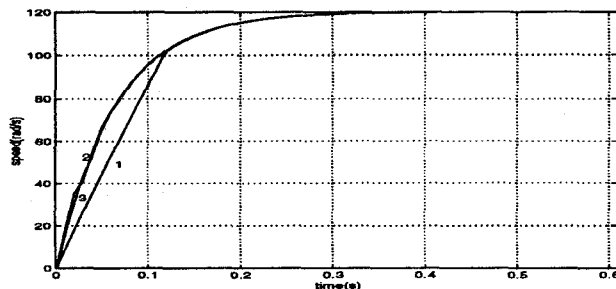


Figure 15: Curve 1 shows the speed response with parameter Set 1. Curve 2 shows the speed response for a IMRAC with parameter Set 2. Curve 3 shows the speed response for a IMRAC with parameter Set 3.

6. Conclusions

Table 1 summarizes the relative results obtained from the simulation of three different adaptive controllers. Adaptability refers to the ability of the controller to cope with varying system parameters. Start up tuning is the initial adjustments to make the algorithm work. The table also evaluates the effects of setpoint and load disturbances, complexity of the controllers and their performances at the small sampling rates. As seen from the table, parameter estimation and adaptation is difficult when the parameters changes are fast with the IMRAC.

DMRAC gives good results with load, setpoint and parameter disturbances. Care is needed in the start up tuning for the DMRAC. The control saturation problem is addressed and the suggested solution to this nonlinear effect is simulated. The controller maintained the model following while the current commands remained within their specified limits. By virtue of its independence of parameter estimation methods and controller redesign requirements, the DMRAC is simpler to implement than the IMRAC.

Acknowledgments

This paper is partially based upon research performed under NSF Grant ECS-9413123.

References

- [1] T.J.E. Miller, "Brushless Permanent-Magnet and Reluctance Motor Drives," Clarendon Press, Oxford 1989.
- [2] D. C. Hanselman, "Brushless Permanent-Magnet Motor Design," McGraw-Hill, Inc., 1994.
- [3] R. B. Sepe and J.H. Lang, "Real-Time Adaptive Control of the Permanent-Magnet Synchronous Motors," IEEE Trans. Ind. Appl., Vol.27, No.4, pp. 706-714, 1991.
- [4] E. Unkauf and D.A. Torrey, "Direct Model Reference Control of an Induction Motor," Proc. of the IEEE Applied Power Electronics Conf., pp. 192-196, Dallas, TX, 1995.
- [5] P. Pillay and R. Krishnan, "Modelling, Simulation, and Analysis of Permanent-Magnet Motor Drives," IEEE Trans. Ind. Appl., Vol.25, No.2, pp. 265-278, 1989.
- [6] F.M. El-Khouly, A.S. Abdel-Ghaffar, A.A. Mohammad and A.M. Sharaf, "A.I. speed control strategies for permanent magnet dc motor drives," in Proc. IEEE Ind. Appl. Soc. Ann. Meeting, pp.379-385, 1994.
- [7] H. Kaufman, I. Bar-kana, and K.M. Sobel, "Direct Adaptive Control Algorithms: Theory and Applications," Springer-Verlag, New York, 1994.
- [8] I.D. Landau and R. Liozano, "Unification of discrete time explicit model reference adaptive control designs," Automatica, 17, 593-611, 1981
- [9] A. O. Chingcuanco, P. M. Lubin, P. R. Meinhold, M. Tomizka. "Model reference adaptive control for the azimuth-pointing system of a balloon-borne stabilized platform," International Journal of Adaptive Control and Signal Processing, Vol.5, 107-120, 1991

Appendix

PMBDC motor parameters:

$$\begin{aligned}
 J &= 0.001525 \text{ Kg}m^2. \\
 B &= 0.0008015 \text{ Nm/rad/s.} \\
 K_v &= 0.1987465 \text{ Nm/A.} \\
 L - M &= 0.00929 \text{ H.} \\
 R &= 4 \ \Omega.
 \end{aligned}$$